



Discussion of a variant of eccentric drives utilizing rolling elements

S. Fritsch¹ · S. Landler¹ · M. Otto¹ · B. Vogel-Heuser² · M. Zimmermann³ · K. Stahl¹

Received: 17 February 2023 / Accepted: 5 July 2023 / Published online: 26 July 2023
© The Author(s) 2023

Abstract

In this paper a variant of eccentric drives will be described, which uses rolling elements instead of an eccentric gear. These rolling elements are constrained by a concentric carrier allowing for radial movement and are moved by an eccentric crank. They mesh with a gear geometry that translates their radial movement into tangential movement and constrains their position. Multiple offset eccentricities may be used with the same gear to reduce occurring forces. Such a drive may prove easier to manufacture than currently used eccentric drives, but the characteristics are not yet fully researched. The components and the working principle of such a drive will be described, and consistent names for the components will be established in this paper. Using these the movement of the rolling elements and the resulting gear geometry will be mathematically described. The forces on a singular rolling element will be derived. An overview of and comparison with related drive mechanisms will be given to aid in the classification of this drive. Different variations of this drive will be discussed, including the choice of rolling elements, whether to use an external or internal gear, and whether a direction-reversing or non-direction-reversing drive is advantageous.

Untersuchung einer Variante von Exzentergetrieben mit Wälzkörpern

Zusammenfassung

In dieser Arbeit wird eine Variante von Exzentergetrieben beschrieben, die Wälzkörper, statt einem exzentrisch laufenden Zahnrad verwendet. Die Wälzkörper werden durch einen konzentrisch laufenden Träger gehalten, der Radialbewegung zulässt, und durch eine exzentrische Kurbel bewegt. Sie greifen in eine Zahnradgeometrie ein, die ihre radiale Bewegung in eine tangentielle Bewegung umwandelt und ihre Position festlegt. Zur Verringerung der auftretenden Kräfte können mehrere versetzte Exzentrizitäten mit demselben Zahnrad verwendet werden. Dieses Getriebe könnte sich als einfacher herzustellen erweisen als die derzeit verwendeten Exzenterantriebe, aber die Eigenschaften sind noch nicht vollständig erforscht.

✉ S. Fritsch
simon.fritsch@tum.de

¹ TUM School of Engineering and Design, Department of Mechanical Engineering, Gear Research Center (FZG), Munich Institute of Robotics and Machine Intelligence (MIRMI), Technical University of Munich, Boltzmannstr. 15, 85748 Garching, Germany

² TUM School of Engineering and Design, Department of Mechanical Engineering, Institute of Automation and Information Systems, Munich Institute of Robotics and Machine Intelligence (MIRMI), Technical University of Munich, Boltzmannstr. 15, 85748 Garching, Germany

³ TUM School of Engineering and Design, Department of Mechanical Engineering, Laboratory for Product Development and Lightweight Design, Munich Institute of Robotics and Machine Intelligence (MIRMI), Technical University of Munich, Boltzmannstr. 15, 85748 Garching, Germany

In dieser Arbeit werden die Komponenten und das Funktionsprinzip eines solchen Antriebs beschrieben und einheitliche Bezeichnungen für die Komponenten festgelegt. Mit diesen wird die Bewegung der Wälzkörper und die daraus resultierende Getriebegeometrie mathematisch beschrieben und die Kräfte auf einen einzelnen Wälzkörper berechnet. Zur Einordnung dieses Getriebes wird ein Überblick über und Vergleich mit verwandten Antrieben gegeben. Es werden verschiedene Varianten dieses Getriebes diskutiert, darunter die Wahl der Wälzkörper, die Entscheidung zwischen Außen- und Innenverzahnung und die Frage, ob ein drehrichtungsumkehrender oder drehrichtungsbeibehaltender Aufbau von Vorteil ist.

1 Introduction

Robotic systems have become an integral part of modern life. More and more companies utilize robot-like systems to reduce cost, increase production speed, and protect workers from having to perform hazardous activities. The increased adaptation of such systems has reduced their price significantly. For robotic systems structural components and control electronics have become cheaper and cheaper, but the actuators remain a major cost driver. High torque motors are heavier, more expensive and need higher currents to operate. This leads to a demand for cheap lightweight drive systems that offer high transmission ratios to reduce requirements on the motor [1–3].

This need has often been filled by eccentric drives, such as cycloidal and strain wave drives [4]. This paper discusses a type of eccentric drive, which uses rolling elements as a power transmitting element. Drives with a similar structure have been patented in the past [5, 6], but the mathematical description and scientific discussion of the topic has been lacking.

By using commonly available and easily mass-produced rolling elements this drive could be easier to manufacture than traditional eccentric drives, while preserving their advantages, such as low backlash, concentric input and output and high transmission ratios, while remaining backdrivable. Many of the force transmitting components can be build using readily available metal components, enabling an easy

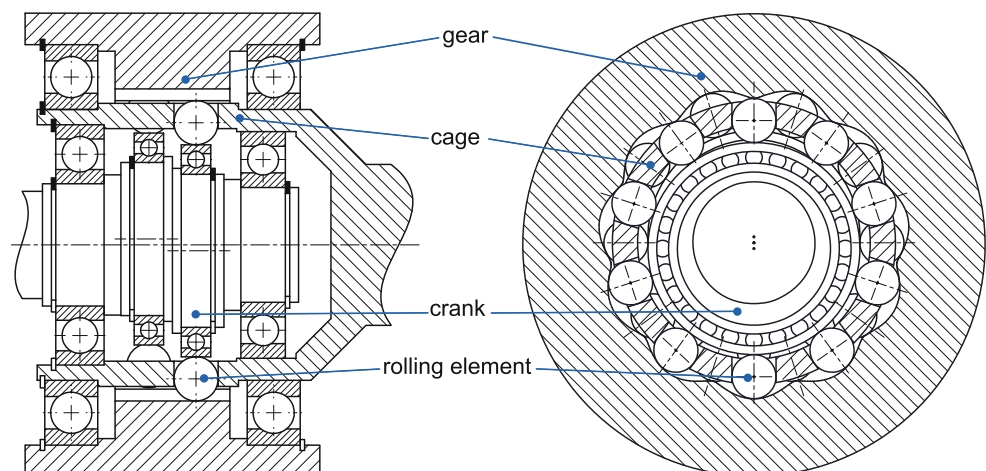
composite construction of the drive. This paper presents a mathematical description and scientific discussion of such drives. Different variants on the kinematic will be presented and discussed.

The use of drives with new geometries and novel materials in robots is also being researched in the project DSL4RAS [1]. This paper is part of this project.

2 Description of components and working principle

An exemplary design of a rolling element eccentric drive can be seen in Fig. 1. This structure is similar to some patents [5, 6] but was developed independently from those. This drive works by pressing rolling elements into the profile of an outer gear by means of a crank. The gear is designed such that the rolling elements are constrained radially between the crank and the gear profile at all points of their path. Such a gear leads to a state, in which all rolling elements that are driven by the crank are pushed into a “ramp” translating the radial force from the crank into a tangential force. No friction is needed for this power transmission. At the same time the rolling elements are constrained by a cage that spaces them evenly around the axis of rotation. This cage is named so in reference to common bearing nomenclature [7]. The cage also pushes the rolling elements which are not driven by the crank along their path.

Fig. 1 Rolling element eccentric drive with $i = -10$ and two eccentricities offset by 180°



To use this drive for speed reduction the crank has to be used as the input and the outer gear or cage can be used as the output, whilst the other provides a fixed reference.

Different types of rolling elements can be used in this drive without changing the core functionality. This paper assumes the rolling elements to have a circular cross section. The advantages and disadvantages of different types of rolling elements will be discussed in Sect. 5. The size of the rolling elements puts a limit on the maximum eccentricity of the crank, as the crank must stay in contact during the outermost part of their path and center of the rolling element must stay inside the cage during the innermost part to stay constrained. Ignoring the curvature of the cage and needed tolerances between parts, both of which further reduce the maximal eccentricity, we can derive, that the eccentricity must be smaller than half the radius of the rolling elements.

$$e < \frac{b}{2} \tag{1}$$

A bearing can be used as the contacting surface of the crank. It reduces sliding friction, that would normally occur between the crank and the rolling elements. This is especially critical, because this contact has high virtual power, as it consists of both high forces and high relative speeds [8]. Using a bearing on the crank also provides a convenient hardened and precise surface for the rolling elements to roll on. Multiple offset eccentricities can be used with the same gear by offsetting the position of the rolling elements in the cage. A crank with more than one eccentricity is advantageous, as it balances occurring static forces and reduces dynamic forces.

The kinematics of the drive do not restrict the achievable transmission ratio. In practice the transmission ratio is limited by multiple engineering considerations, such as the minimal size of the rolling elements, the overall size of the drive and the permissible degree of intersection of the gear geometry. These effects can lead to skipping between possible positions under load.

Backlash occurs between the rolling elements and the cage and between the rolling elements and the gear. The backlash between the rolling elements and the cage can be easily calculated and minimized using a standard fit. The backlash between the rolling elements and the gear is more complicated to calculate and is beyond the scope of this paper. Backlash can be reduced or even eliminated by choosing closer fits or by slightly offsetting the angle of multiple eccentricities relative to each other, similar to cycloidal drives [4]. The manufacturing tolerances have a strong influence on the achievable backlash. Very tight tolerances may lead to jamming of the rolling elements.

3 Description of geometry and forces

3.1 Geometric derivation

In the following the geometry of the outer gear will be derived. The nomenclature is based on the work of Lehmann [9], due to the similarity to cycloidal curves. It should be noted however, that the generated curves are not cycloids, because the rolling condition is not fulfilled. The geometric model used for the following derivation can be seen in Fig. 2.

We can derive the length of c for any given β by considering the triangle formed by e , $a + b$, and c , as seen in Fig. 3.

Using simple trigonometric identities, we can calculate the distance c :

$$h = e \cdot \sin(\beta) \tag{2}$$

$$c = \sqrt{e^2 - h^2} + \sqrt{(a + b)^2 - h^2} \tag{3}$$

$$c = \sqrt{e^2 - e^2 \cdot \sin^2(\beta)} + \sqrt{(a + b)^2 - e^2 \cdot \sin^2(\beta)} \tag{4}$$

$$c = e \cdot \cos(\beta) + \sqrt{(a + b)^2 - e^2 \cdot \sin^2(\beta)} \tag{5}$$

We can also calculate the pressure angle between the crank and the rolling element δ from this triangle:

$$(a + b) \sin(\delta) = h \tag{6}$$

$$\delta = \arcsin\left(\frac{e}{a + b} \sin(\beta)\right) \tag{7}$$

The path of the rolling elements is expressed in polar coordinates by the radius c and the angle α . We can also express them in cartesian coordinates:

$$\vec{c} = \left(e \cos(\beta) + \sqrt{(a + b)^2 - e^2 \sin^2(\beta)} \right) \cdot \begin{pmatrix} \cos(\alpha) \\ \sin(\alpha) \end{pmatrix} \tag{8}$$

The relation between α and β can be derived by considering the intended transmission ratio of i . For this the transmission from the crank to the cage, relative to a fixed gear will be considered. The input angle is given by:

$$\phi_{\text{input}} = \phi_{\text{crank}} = \alpha + \beta \tag{9}$$

The output angle is given by:

$$\phi_{\text{output}} = \phi_{\text{cage}} = \alpha \tag{10}$$

Fig. 2 Mathematical model for the derivation of the gear geometry

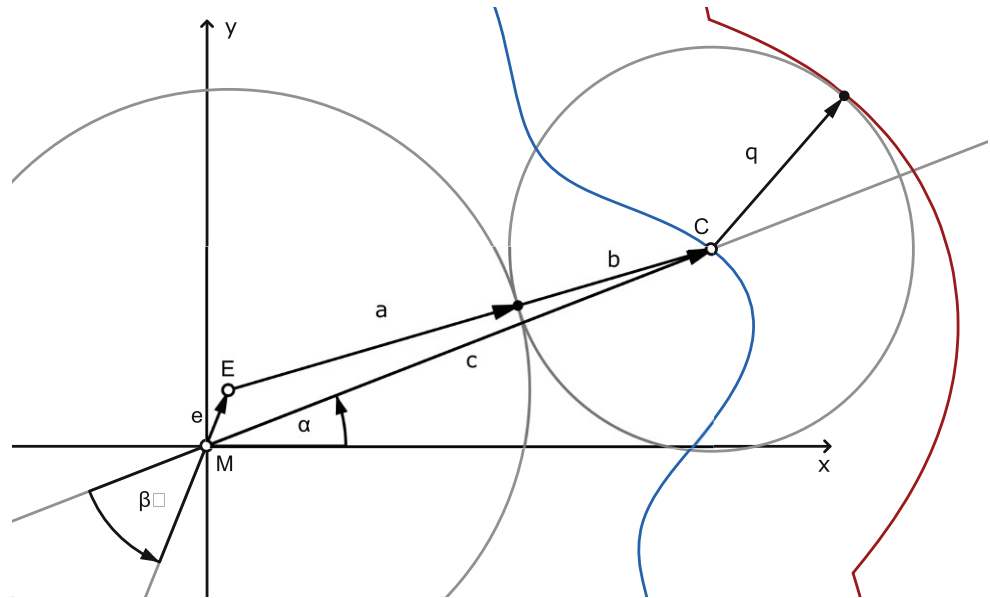
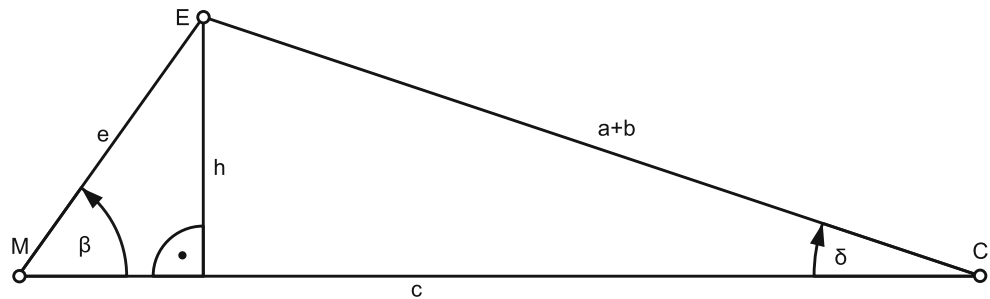


Fig. 3 Isolated triangle for the derivation of the rolling elements path



The transmission ratio i is defined to be:

$$i = \frac{\phi_{\text{input}}}{\phi_{\text{output}}} = \frac{\alpha + \beta}{\alpha} \tag{11}$$

This leads to:

$$i \cdot \alpha = \alpha + \beta \tag{12}$$

$$\alpha = \frac{\beta}{i - 1} \tag{13}$$

By considering that one full rotation of β leads back to the same point on the tooth profile we can get the tooth count:

$$\pm z \cdot \alpha = \beta \tag{14}$$

This leads to:

$$\pm z = i - 1 \tag{15}$$

Due to the symmetry of the generated curve, we can generalize for negative transmission ratios:

$$z = |i - 1| \tag{16}$$

The motion equation for arbitrary inputs can be derived by considering that the angle of the cage is equal to the sum of the angle of the gear and the relative angle between the gear and the crank times the transmission ratio i :

$$\phi_{\text{cage}} = (\phi_{\text{crank}} - \phi_{\text{gear}}) \cdot i + \phi_{\text{gear}} \tag{17}$$

$$0 = \phi_{\text{crank}} \cdot i + \phi_{\text{gear}} \cdot (1 - i) - \phi_{\text{cage}} \tag{18}$$

This equation is analogous to the Willis equation for planetary gears [10].

In the following the tooth count will be used to define the curves, because one curve can be described by more than one transmission ratio. For example, the curves for $i = -6$ and $i = 8$ are identical.

Which of those outputs is achieved with a given gear is determined by the theoretical number of rolling elements n_{theo} . If it is one less than the teeth count the gearing will reverse direction, if it is one more than the teeth count it will not reverse direction. The theoretical number of rolling

elements dictates the positions where rolling elements can be for the drive to still turn. For a successful operation of the drive not all these positions have to be filled. Under most circumstances an equal spacing of rolling elements is still desired, which leads to possible actual numbers of rolling elements being the factors of n_{theo} .

$$n_{\text{theo}} = k \cdot n_{\text{actual}}, k \in \mathbb{N} \tag{19}$$

As n_{theo} can be high enough to cause overlap between the rolling elements for high transmission ratios an actual number of rolling elements lower than the theoretical is often necessary. The actual number of rolling elements has to be high enough to ensure a sufficient number of elements in driving contact during all positions of the drive.

Plugging in the above derived relation between α and β we get:

$$\vec{c}(\beta) = \begin{pmatrix} e \cos(\beta) + \sqrt{(a+b)^2 - e^2 \sin^2(\beta)} \\ \cos\left(\frac{1}{z}\beta\right) \\ \sin\left(\frac{1}{z}\beta\right) \end{pmatrix} \tag{20}$$

The curve $\vec{c}(\beta)$ represents the path the centres of the rolling elements follow during the operation of the mechanism. It is noteworthy, that the path of the rolling elements does not individually depend on a or b, but only on their sum.

To get the geometry of the gear we need to calculate the outer equidistant of the path. The outer equidistant can be calculated using the outwards pointing normal vector of the curve, which in turn can be derived from the tangent vector. The tangent vector $\vec{t}(\beta)$ of the curve can be calculated by differentiating with respect to the parameter of the curve β [11]:

$$\vec{t}(\beta) = \frac{d\vec{c}}{d\beta} = \begin{pmatrix} -e \sin(\beta) - \frac{e^2 \sin(\beta) \cos(\beta)}{\sqrt{(a+b)^2 - e^2 \sin^2(\beta)}} \\ \cos\left(\frac{1}{z}\beta\right) \\ \sin\left(\frac{1}{z}\beta\right) \end{pmatrix} \cdot \begin{pmatrix} e \cos(\beta) + \sqrt{(a+b)^2 - e^2 \sin^2(\beta)} \\ \frac{1}{z} \cdot \begin{pmatrix} -\sin\left(\frac{1}{z}\beta\right) \\ \cos\left(\frac{1}{z}\beta\right) \end{pmatrix} \end{pmatrix} \tag{21}$$

$$\vec{t}(\beta) = \frac{d\vec{c}}{d\beta} = \frac{c}{z} \cdot \begin{pmatrix} -\sin\left(\frac{1}{z}\beta\right) \\ \cos\left(\frac{1}{z}\beta\right) \end{pmatrix} - e \sin(\beta) \left(1 + \frac{e \cos(\beta)}{\sqrt{(a+b)^2 - e^2 \sin^2(\beta)}} \right) \cdot \begin{pmatrix} \cos\left(\frac{1}{z}\beta\right) \\ \sin\left(\frac{1}{z}\beta\right) \end{pmatrix} \tag{22}$$

From here the normal vector can be calculated by finding a vector, that is orthogonal to $\vec{t}(\beta)$:

$$\vec{n}(\beta) = \pm \begin{pmatrix} -t_y \\ t_x \end{pmatrix} \tag{23}$$

$$\vec{n} = \pm \begin{pmatrix} \frac{c}{z} \cdot \begin{pmatrix} -\cos\left(\frac{1}{z}\beta\right) \\ -\sin\left(\frac{1}{z}\beta\right) \end{pmatrix} \\ -e \sin(\beta) \left(1 + \frac{e \cos(\beta)}{\sqrt{(a+b)^2 - e^2 \sin^2(\beta)}} \right) \\ \begin{pmatrix} -\sin\left(\frac{1}{z}\beta\right) \\ \cos\left(\frac{1}{z}\beta\right) \end{pmatrix} \end{pmatrix} \tag{24}$$

As we want to find the outwards pointing normal vector its x component must be positive at $\beta=0$:

$$n_x(\beta=0) = \pm \left(-\frac{c}{z} + 0 \right) > 0 \tag{25}$$

$$\vec{n} = \frac{c}{z} \cdot \begin{pmatrix} \cos\left(\frac{1}{z}\beta\right) \\ \sin\left(\frac{1}{z}\beta\right) \end{pmatrix} + e \sin(\beta) \left(1 + \frac{e \cos(\beta)}{\sqrt{(a+b)^2 - e^2 \sin^2(\beta)}} \right) \cdot \begin{pmatrix} -\sin\left(\frac{1}{z}\beta\right) \\ \cos\left(\frac{1}{z}\beta\right) \end{pmatrix} \tag{26}$$

Scaling the normal vector down to unit length:

$$\vec{N} = \frac{\vec{n}}{|\vec{n}|} \tag{27}$$

We can now calculate the points of the outer gear:

$$\vec{r} = \vec{c} + q \cdot \vec{N} \tag{28}$$

Without taking tolerances into account, we want the distance of the equidistant to be equal to the radius of the rolling element:

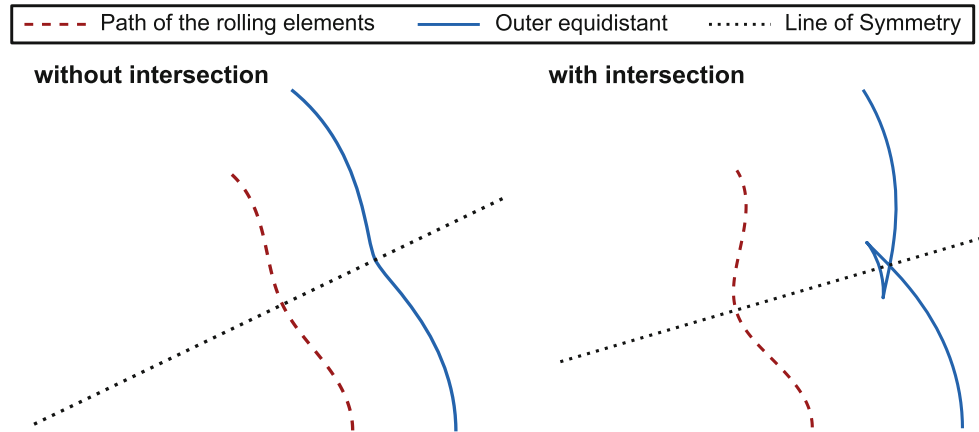
$$q = b \tag{29}$$

$$\vec{r} = \vec{c} + b \cdot \vec{N} \tag{30}$$

The generated curve may intersect itself. For the outer equidistant this happens during the inner portion of the path, when the generated geometry crosses the line of symmetry located at the valley of the rolling elements path. This can be used to calculate the point of intersection efficiently. An example of a curve without and one with self-intersection can be seen in Fig. 4.

This causes play during the affected area of rolling elements path. Rolling elements in this area are very limited in their ability to contribute to the transmission of torque. It also causes the gear to form a sharp peak, that may need to be rounded to prevent it from getting damaged due to the

Fig. 4 Comparison of curves with and without self-intersection



unconstrained movement of the rolling elements and forces from the transmission of torque.

This intersection can be prevented or reduced by increasing the distance of the rolling elements from the eccentric point $a + b$ or reducing the number of teeth z , the eccentricity e , or the distance of the equidistant q , which is mainly given by the radius of the rolling elements b .

Using a curve with intersections reduces the number of rolling elements, that can transmit torque at any one point. Despite that this play on the inner sections of the curve may be beneficial as it reduces constraining forces during a section, that is not well conditioned for transmitting torque.

3.2 Derivation of forces

Using the above derived geometry, we can calculate the pressure angle between the rolling elements and the outer gear:

$$\gamma = \angle(\vec{n}, \vec{c}) \tag{31}$$

Using:

$$\angle(\vec{c}, \vec{e}_x) = \alpha \tag{32}$$

We get:

$$\gamma = \angle(\vec{n}, \vec{e}_x) - \alpha \tag{33}$$

$$\gamma = \arccos\left(\frac{\vec{n} \cdot \vec{e}_x}{|\vec{n}| |\vec{e}_x|}\right) - \alpha \tag{34}$$

$$\gamma = \arccos\left(\frac{n_x}{|\vec{n}|}\right) - \alpha = \arccos(N_x) - \alpha \tag{35}$$

We can now calculate the resulting forces on a rolling element from the torque transmitted by it. Calculating the distribution of torque on multiple rolling elements is beyond the scope of this paper. In Fig. 5 a free body diagram for one rolling element is shown for a direction-reversing and a non-direction-reversing drive. To account for the different direction of the crank force, the pressure angle δ is defined to be negative for direction-reversing drives.

Assuming negligible acceleration forces on the rolling element we can use the static force equilibrium:

$$\Sigma \vec{F} = 0 \tag{36}$$

$$\vec{F}_{\text{crank}} + \vec{F}_{\text{cage}} + \vec{F}_{\text{gear}} = 0 \tag{37}$$

In the y direction we get:

$$F_{\text{crank},y} = \sin(\delta) \cdot F_{\text{crank}} \tag{38}$$

$$F_{\text{gear},y} = \sin(\gamma) \cdot F_{\text{gear}} \tag{39}$$

$$F_{\text{cage},y} = -F_{\text{cage}} \tag{40}$$

$$\Sigma F_y = \sin(\delta) \cdot F_{\text{crank}} + \sin(\gamma) \cdot F_{\text{gear}} - F_{\text{cage}} = 0 \tag{41}$$

Similarly, we get in the x direction:

$$\Sigma F_x = \cos(\gamma) \cdot F_{\text{gear}} - \cos(\delta) \cdot F_{\text{crank}} = 0 \tag{42}$$

Solving for the force on the crank:

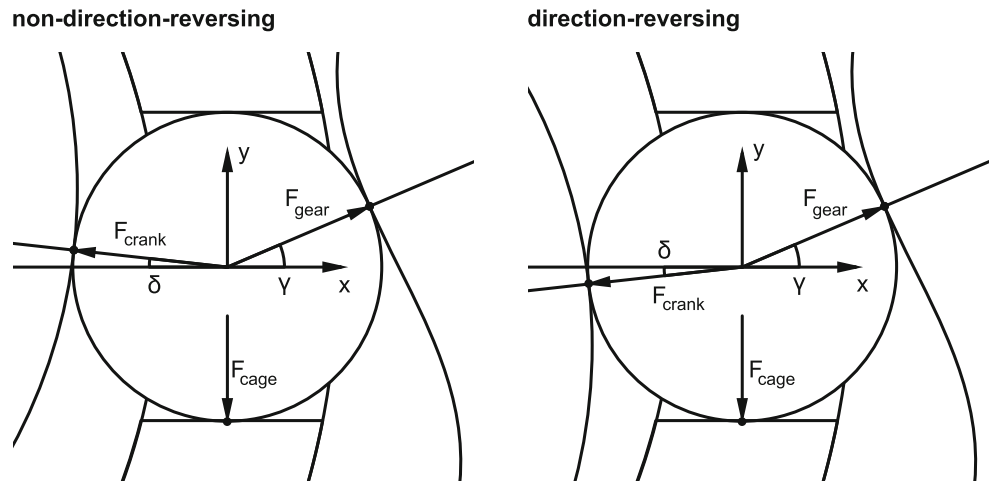
$$F_{\text{crank}} = \frac{\cos(\gamma)}{\cos(\delta)} \cdot F_{\text{gear}} \tag{43}$$

We can now plug this equation into Eq. 41:

$$\cos(\gamma) \cdot \frac{\sin(\delta)}{\cos(\delta)} \cdot F_{\text{gear}} + \sin(\gamma) \cdot F_{\text{gear}} = F_{\text{cage}} \tag{44}$$

$$F_{\text{gear}} = \frac{1}{\cos(\gamma) \tan(\delta) + \sin(\gamma)} F_{\text{cage}} \tag{45}$$

Fig. 5 Free body diagram for the direction-reversing and non-direction-reversing variant



With a given output Torque T_{out} from one rolling element we can calculate the force on the cage:

$$F_{cage} = \frac{T_{out}}{c} \tag{46}$$

$$F_{gear} = \frac{1}{\cos(\gamma) \tan(\delta) + \sin(\gamma)} \frac{T_{out}}{c} \tag{47}$$

As both γ and δ go towards zero for both the peaks and valleys the theoretical resulting force goes towards infinity for those positions. The actual resulting force is determined, among other things, by the stiffness of the mechanism.

4 Classification

The rolling elements eccentric drive shows a lot of similarity with other eccentric drives, such as strain wave gearing, cycloidal drives, and the Galaxie® drive. This similarity becomes more apparent, when you consider the totality of the rolling elements as a second gear. This gear is analogous to the flex spline of a strain wave drive or the cycloidal disk of a cycloidal drive. As opposed to those gears the rolling elements are not one body and must stay in contact with the outer gear to stay geometrically constrained. In addition, the rolling elements can rotate along their path, which reduces friction.

In comparison to strain wave drives the rolling element eccentric drive has a lower manufacturing and design complexity, as it does not require a flex spline. Strain wave drives on the other hand are not limited in the usable eccentricity by the size of the rolling elements and can achieve higher transmission ratios due to the smaller teeth [12, 13].

Cycloidal drives are similar in a multitude of ways. For one the generated gear geometries look similar to cycloidal curves and are derived in a similar way. Unfortunately, this similarity does not lead to an equivalence, as cycloidal

curves are generated using the rolling of two circles on each other, which sets the relative movement of the base and rolling circle. In the rolling element eccentric drive however, this relative movement is set artificially to achieve the desired transmission ratio and does not fulfil the rolling condition. For this reason, the generated curves are not cycloidal in nature. Cycloidal drives also offer similar achievable transmission ratios. The ring pins of a cycloidal drive can be built to rotate which reduces losses in a similar way the rotation of the rolling elements. A general comparison of the manufacturing complexity of both drives is difficult, as it heavily depends on the specific design of both drives [13, 14].

The Galaxy® drive is another eccentric drive, that uses singular teeth instead of a second gear. In the galaxy drive these teeth are pins with tooth profiles on the end instead of the rolling elements of the herein discussed drive. This provides optimized contact parameters, a higher achievable transmission ratio and does not limit the eccentricity, but it also leads to a significantly higher manufacturing complexity and does not allow for rotation to reduce sliding friction [15, 16].

There are a number of patents for similar mechanisms. The closest among these is a drive mechanism patented by Wilhelm Vogt [5] in 1919. He describes the drive kinematic of a rolling element eccentric drive and shows examples of variants with internal and of variants with external gears. In his patent he does not precisely describe the geometry of the gear, only describing them in general terms. He only names the drive as a “transmission gearbox” and does not classify it as an eccentric drive. No further publication or record of his work besides his patents could be found.

Another similar drive mechanism was patented in 1986 by Ren Zhu Shao [17]. It uses pins with rollers on both ends, which results in a similar gear geometry. The “Harmonic Drive Antriebs GmbH” patented a similar drive in 1990.

This drive uses a straight tooth profile which does not fully constrain the rolling elements [6].

5 Discussion of different variants

There are multiple possible variations on the principle of the rolling element eccentric drive, which provide different characteristics. In this section some of these will be discussed, as well as their advantages and disadvantages.

One important design consideration is the choice of rolling elements. In principle many different types could be used. This paper will focus on cylindrical rollers and balls, but other types are thinkable. Cylindrical rollers have the advantage of linear contact providing higher stiffness and enabling higher forces. On the other hand, this also complicates the manufacturing of the cage and necessitates consideration of the contact on the flat side of the cylinder. Edge loading may occur due to imprecise alignment of the components or deformation under load. Balls are cheaper and facilitate using a cage with simple circular holes, as opposed to the more complicated rectangular holes needed for cylindrical rollers. They have the disadvantage of point contact and as such lower stiffness and transmittable torque [18].

Another design consideration is whether to use a gear with one tooth more than the theoretical number of rolling elements or one with one tooth less. Both provide the same transmission ratio, when using the cage as the output. When using the gear as the output a similar design consideration must be made for the number of rolling elements. If the gear has one tooth less than the number of rolling elements the output will turn in the same direction as the input. If it has one tooth more than the number of rolling elements the output will turn in the opposite direction to the input. The direction reversing variant of the gear, with one tooth more than the transmission ratio leads to a closer osculation between the rolling elements and the gear. This leads to a bigger equivalent radius of curvature resulting in better contact parameters [19]. The additional two teeth also cause the gear to tend towards more self-intersection, which can reduce the average number of rolling elements in contact. A more in-depth analysis of the forces and stiffnesses occurring is necessary to decide which variant is advantageous.

This paper so far has been focused on a variation of this mechanism, that uses an inner crank and an outer gear. It is however possible to produce the inverse variation of this, in which the crank is the outermost part, and an inner external gear is used, as seen in Fig. 6. For this to work a hollow shaft with an eccentric central hole has to be used as the crank. The path of the rolling elements stays largely the same, but the radius of the rolling elements b has to be

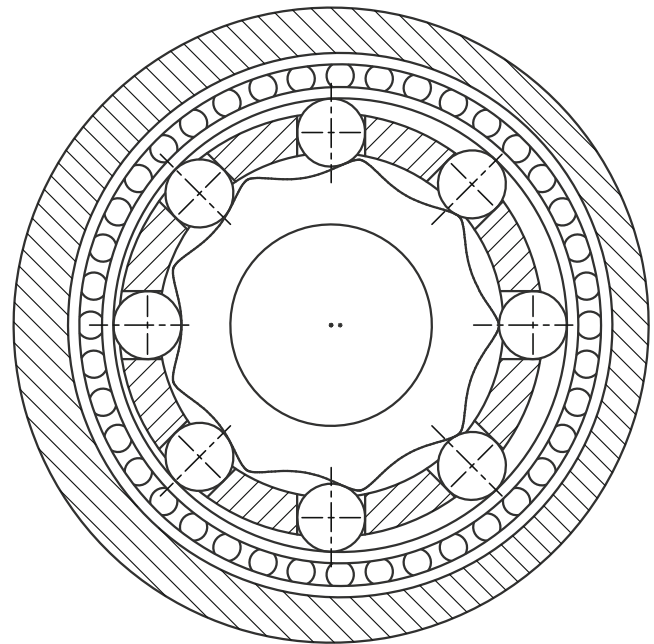


Fig. 6 Rolling element eccentric drive with an inner gear and outer crank with $n=8$, $z=9$

subtracted from the radius of the crank a , instead of being added to it:

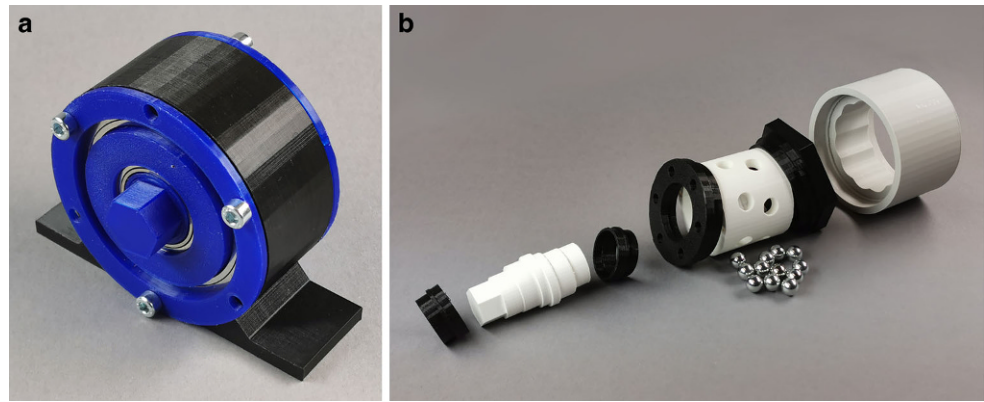
$$(a + b) \rightarrow (a - b) \quad (48)$$

The geometry of the now needed external inner gear is derived from the inner equidistant of the path of the rolling elements, which we get by subtracting the normal vector instead of adding it:

$$\vec{r} = \vec{c} - q \cdot \vec{N} \quad (49)$$

The main advantage of this variation is, that it uses an external instead of an internal gear. This promises better manufacturability of the gear, due to the easier access for tooling [20]. The main drawback of this variation is, that the input has to be the outermost part of the drive. This is unusual for such drives and might lead to difficulties with the integration into existing actuator designs. It also causes the drive to have higher rotational inertia, as the high-speed input side now consists of the larger and heavier outer part of the gearing. This is doubly so if bearings are used on the contact surface, as they not only have to be larger to account for the necessarily bigger crank radius but also have to account for now using their inner instead of their outer diameter as the relevant radius. This leads to a major increase in the required bearing size and with that weight and inertia. The advantages in manufacturability are largely not present, when 3D printing the mechanism, while the weight increase of the bearings is even more significant in relation

Fig. 7 Assembled prototype (a) and disassembled 3D printed parts and rolling elements (b)



to the lightweight printed parts. For manufacturing a metal version of the mechanism these advantages are more present and a bearing might not be necessary on the crank causing the inverse variation to have more merit. A combination of the standard and inverse variant could make for a compact two stage reducer, as the gear of one can be joined with the crank of the other, while a combined cage for both provides static reference.

Another possible variation is using a noncircular crank. This would make it possible to incorporate multiple eccentricities or further optimize the contact parameters and gear geometry. A variant with two or more eccentricities on the same set of rolling elements would reduce forces and moments resulting from the power transmission and enable a shorter design. Deviating from a circular crank would however significantly increase the difficulty in manufacturing it and hamper the use of standard bearings on it.

6 Conclusion

In this paper the concept of rolling element eccentric drives was described and the required geometric equations were derived. The classification of this mechanism was discussed and different possible variations on it were introduced. Multiple successful prototypes have been manufactured using FFF-3D-printing as seen in Fig. 7.

Nonetheless are there still multiple open questions, such as the distribution of force on multiple rolling elements, which will have to be answered before the viability of such a drive can be evaluated. Many important characteristics of this drive, such as backlash and stiffness have not yet been researched. The influence of manufacturing characteristics on the performance of the drive is still open for further research. Further research into the force distribution between the rolling elements utilizing the contact geometry and forces established in this paper can provide better estimates for the achievable power density and stiffness of this drive concept. An analysis of dynamic forces in combi-

Table 1 Nomenclature

a	Radius of the crank
b	Radius of the rolling elements
e	Eccentricity of the crank
c	Distance from the center of rotation to the center of the rolling element
i	Transmission ratio from crank to cage
z	Number of created curve sections in one full rotation/teeth count
q	Distance of the equidistant used as the outer gear
n_{theo}	Theoretical number of rolling elements
n_{actual}	Actual number of rolling elements
F_{cage}	Force between the rolling elements and the cage
F_{crank}	Force between the rolling elements and the crank
F_{gear}	Force between the rolling elements and the gear
$F_{[...],x/y}$	x/y-component of a force
T_{out}	Transmitted output torque of a rolling element
<i>Vectors and Points</i>	
M	Centre of rotation of the drive
C	Centre of a rolling element
E	Centre of the eccentricity
\vec{c}	Vector from the center of rotation M to the center of the rolling element C
\vec{t}	Tangent vector of the rolling elements path
\vec{n}	Outward pointing normal vector of the rolling elements path
\vec{N}	Normalized outward pointing normal vector of the rolling elements path
\vec{r}	Vector from the centre of rotation M to a point of the gear geometry
<i>Greek Symbols</i>	
α	Angle of the rolling element
β	Angle between the rolling element and the eccentricity
γ	Pressure angle between the rolling element and the outer gear
δ	Pressure angle between the crank and the rolling element
ϕ_{crank}	Angle of the crank relative to a fixed reference
ϕ_{cage}	Angle of the cage relative to a fixed reference
ϕ_{gear}	Angle of the gear relative to a fixed reference
ϕ_{input}	Angle of the component used as the input relative to a fixed reference
ϕ_{output}	Angle of the component used as the output relative to a fixed reference

nation with the force distribution and stiffness can provide an estimate for the maximum permissible rotational speed. With the help of a domain specific language [1] comparisons with established drives may be simplified.

7 Nomenclature

The nomenclature is shown in Table 1.

Funding The presented results are based on the research project 461993234 supported by the German Research Foundation e. V. (DFG) The authors would like to thank for the sponsorship and support received from the DFG.

Funding Open Access funding enabled and organized by Projekt DEAL.

Conflict of interest S. Fritsch, S. Landler, M. Otto, B. Vogel-Heuser, M. Zimmermann and K. Stahl declare that they have no competing interests.

Open Access This article is licensed under a Creative Commons Attribution 4.0 International License, which permits use, sharing, adaptation, distribution and reproduction in any medium or format, as long as you give appropriate credit to the original author(s) and the source, provide a link to the Creative Commons licence, and indicate if changes were made. The images or other third party material in this article are included in the article's Creative Commons licence, unless indicated otherwise in a credit line to the material. If material is not included in the article's Creative Commons licence and your intended use is not permitted by statutory regulation or exceeds the permitted use, you will need to obtain permission directly from the copyright holder. To view a copy of this licence, visit <http://creativecommons.org/licenses/by/4.0/>.

References

- Vogel-Heuser B, Zimmermann M, Stahl K, Land K, Ocker F, Rötzer S, Landler S, Otto M (2020) Current challenges in the design of drives for robot-like systems. In: IEEE International Conference on Systems, Man, and Cybernetics (SMC), pp 1923–1928 <https://doi.org/10.1109/SMC42975.2020.9282988>
- Sanneman L, Fourie C, Shah J (2021) The state of industrial robotics: emerging technologies, challenges, and key research directions
- Braun J, Archer MS, Reichberg GM, Sánchez Sorondo M (eds) (2021) Robotics, AI, and humanity: science, ethics, and policy, 1st edn. Springer, Cham
- Rosenbauer T (1994) Getriebe für Industrieroboter: Beurteilungskriterien, Kenndaten, Einsatzhinweise (Dissertation, RWTH Aachen)
- Vogt W (1921) DE338495C Übersetzungsgetriebe. <https://worldwide.espacenet.com/patent/search?q=pn%3DDE338495C>. Accessed 27 Jan 2023
- N.N. (1990) DE3906053A1 Getriebe nach Art eines Spannungswellengetriebes. <https://worldwide.espacenet.com/patent/search?q=pn%3DDE3906053A1>. Accessed 27 Jan 2023
- International Organization for Standardization (2019) ISO 5593: 2019 Rolling bearings—Vocabulary
- García PL, Crispel S, Saerens E, Verstraten T, Lefeber D (2020) Compact gearboxes for modern robotics: a review. *Front Robot Ai*. <https://doi.org/10.3389/frobt.2020.00103>
- Lehmann M (1981) Die Beschreibung der Zykloiden, ihrer Äquidistanten und Hüllkurven: unter besonderer Berücksichtigung der Planeten-Getriebe mit Zykloiden-Kurvenscheiben
- Vullo V (2020) Gears: volume 1: geometric and kinematic design vol 10. Springer, Cham
- Karpfinger C (2017) Höhere Mathematik in Rezepten. Springer, Berlin, Heidelberg
- Routh B (2018) Design aspects of harmonic drive gear and performance improvement of its by problems identification: A review. *AIP Conf Proc*. <https://doi.org/10.1063/1.5029592>
- Pham AD, Ahn HJ (2018) High precision reducers for industrial robots driving 4th industrial revolution: State of arts, analysis, design, performance evaluation and perspective. *Int J Precis Eng Manuf Green Technol* 5:519–533. <https://doi.org/10.1007/s40684-018-0058-x>
- Chang LC, Tsai SJ, Huang CH (2022) Contact characteristics of cycloid planetary gear drives considering backlashes and clearances. *Forsch Ingenieurwes* 86:337–356. <https://doi.org/10.1007/s10010-021-00535-1>
- Schreiber H, Röthlingshöfer T (2017) Kinematic classification of a gearbox comprising separate thrust teeth and its advantages regarding existing approaches. In: International Conference on Gears, 13.–15.09.2017, Garching
- Wimmer T, Schreiber H, Burger T (2015) High torque, torsional stiff and precise: The Galaxy-kinematics. In: International Conference on Gears, 05.–07.10.2015, Garching
- Ren ZS (1986) EP0196650A1 Übertragungseinheit. <https://worldwide.espacenet.com/patent/search?q=pn%3DEP0196650A1>. Accessed 27 Jan 2023
- Niemann G, Winter H, Höhn BR, Stahl K (2019) Konstruktion und Berechnung von Verbindungen, Lagern, Wellen, 5th edn. Maschinenelemente, vol 1. Springer, Berlin, Heidelberg
- Geitner M, Zornek B, Hoja S, Tobie T, Stahl K (2021) Investigations on the micro-pitting and wear behavior of nitrided internal gears. *IOP Conf Ser Mater Sci Eng*. <https://doi.org/10.1088/1757-899X/1097/1/012005>
- Niemann G, Winter H (2003) Getriebe allgemein, Zahnradgetriebe – Grundlagen, Stirnradgetriebe, 2nd edn. Maschinenelemente, vol 2. Springer, Berlin, Heidelberg